*Received: June 10, 2018*
*Revised: June 27, 2018*
*Accepted: June 28,2018*



# Keratin Protein Modified Anatase $TiO_2$ Nanoparticle – Characterizations of Protein Functionalized Surface

Weerachon Phoohinkong[1]*, Tita Foophow[1], Udomsak Kitthawee[1]

[1]*Faculty of Science and Technology, Suan Dusit University, Bangkok, 10700, Thailand*

## Abstract

Anatase titanium dioxide ($TiO_2$) nanoparticle surface is modified with Keratin, a protein from swine wool. The protein structure and the modified surface of the $TiO_2$ nanoparticle is investigated. The structure and bonding of the adsorbed protein on $TiO_2$ surface were investigated by Fourier-transform infrared spectroscopy (FT-IR). The surface morphology of hybrid nanocomposite was observed by Field Emission Scanning Electron Microscopy (FESEM). Chemical bonding between protein and titanium dioxide was further investigated by X-ray Photoelectron Spectroscopy (XPS). Electrochemical cyclic voltammetry (CV) was used to characterize the electrochemical behaviour the protein modified $TiO_2$. The protein structure conformation and chemical bonding interaction with $TiO_2$ surface critically depend on the protein concentration. The protein is likely adsorbed via the interactions between the methyl, carbonyl, and amines group on the side chains of random coil secondary structure with the anatase $TiO_2$ surface. The protein has strong bonding to $TiO_2$ surface as evidently observed XPS for an environment bonding change in binding energy and component at O*1s* Ti*2p* and N*1s* region. The electrochemical behaviour of keratin protein modulated anatase $TiO_2$ hybrid material shows significant influence by protein structure and/or protein concentration at the surface.

**Keywords:** Keratin, Titanium dioxide, Anatase, Hybrid materials

## 1. Introduction

Organic-inorganic conjugated nanohybrid presents new superior unique properties for many applications such as drug delivery, cancer imaging, catalyst, energy storage, implant biosensors and bioelectronics [1-4]. However, the interface phenomena on protein structure, surface structure, adsorbed bonding interaction, synthesis, application and characterization of organic protein functionalization of metal oxide nanoparticle surface still require further study [5]. Titanium dioxide ($TiO_2$) is one of the most important semiconductor materials that attracts great interest in many applications due to unique band gap property, resource abundance, chemical and physical stability. In large volume consumption, $TiO_2$ has been widely used as pigment in paint, cosmetic and food industries. For high value applications such as dye-sensitized solar cell, photocatalyst, photoelectrochemical, sensors, biomedical, bioelectronics, battery and supercapacitor, $TiO_2$ has been explored and utilized in form of modified structure and surface functional material [6-8]. $TiO_2$ conjugated with protein biomolecules surprisingly exhibits new functional challenges in many applications [8]. Proteins can interact with $TiO_2$ surface by different ways such as low interaction of ionic bonding, hydrogen bonding, and strong interaction of covalent bonding [5, 9] from cleavage bonding of 3D structure protein, such as cysteine disulfide bonds, hydrogen bonds and ionic bonds on the side protein chain. The bonding interaction between a protein and $TiO_2$ surface highly depends on many factors including protein type, protein structure and conformation, $TiO_2$ surface lattice and morphology structure, $TiO_2$ surface area, protein concentration, temperature and pH. Keratin is a low cost protein waste from feathers and food industry with a high content of cysteine

*Corresponding Author E-mail: p_veerachon@hotmail.com*

disulfide bond, glycine, and serine. These functional groups are suitable for interactions with $TiO_2$ surface to prepare $TiO_2$ protein conjugate hybrid material for the previously mention applications.

In this work, keratin protein adsorption bonding and conformation structure denature at anatase $TiO_2$ surface were investigated by XPS and IR at the amide and methyl group region. The electrochemical performance on cyclic voltammetry as capacitance electrode is also reported.

## 2. Experimental

### *2.1 Chemical and Materials*

Sodium hydroxide (NaOH) derived from Univar, Ajax Finechem Pty Ltd was used as a washing solvent. The commercial anatase $TiO_2$ was purchased from UNILAB, Ajax Finechem Pty Ltd. The swine wool waste was collected from a community enterprise slaughterhouse of grill swine in Samphran district, Nakhon-Pathom province.

### *2.2. Methods*

The Swine wool waste was washed by stirring in water at 60°C for 2 h, stirring in 0.1M NaOH at 60°C for 6 h, and washed by DI water until the pH of the solution was close to neutral. Keratin protein solution was prepared from 2.5 g and 10.0 g of swine wool in 0.5 M NaOH (500 mL). The starting 1.0 g anatase $TiO_2$ was mixed with 50 mL of keratin protein solution under stirring at room temperature for 2 h. The sediment sample was washed several times by DI water and dried at 60°C for 12 h. The prepared anatase $TiO_2$ samples from 2.5 g and 10.0 g of swine wool solution are named as A-2.5Kr and A-10Kr, respectively.

### *2.3 Characterizations*

Surface morphologies of the prepared samples were observed by FESEM (HITACHI-S47000). The IR characteristics of the protein conformation and structures were investigated by FTIR (IRTracer-100 Shimadzu) with 40 scans. Chemical surface bonding environment of the adsorbed keratin protein on $TiO_2$ surface was further studied using XPS (AXIS Ultra DLD, Kratos Analytical, Shimadzu). Electrochemical performance on cyclic voltammetry was conducted by working planar carbon paste electrode 4×5 $mm^2$ VS Ag/AgCl in 1M KCl electrolyte. Approximately 3 mg of active sample was placed at working electrode without using any additive or binder. The cyclic curve data was collected by NOVA 2.1 software with Autolab PGSTAT302N.

## 3. Results and discussion

Fig. 1 shows FESEM images of (a) A-2.5Kr and (c) A-10Kr samples at low magnification to observe overall sample particle morphologies. High magnified images illustrated in (b) A-2.5Kr and (d) A-10Kr reveal surface morphologies modulated by keratin protein. The clean surface was observed indicating that protein structure could be in the primary and/or secondary structure conformation because the 3D tertiary and quaternary structure should show the morphological structure at least in the regime of 5 nm [10, 11].

FTIR analysis of A-2.5Kr and A-10Kr samples compared with the unmodified anatase $TiO_2$ were carried out and the corresponding overview spectra from 500 to 4500 $cm^{-1}$ are exhibited in Fig. 2 (a). FTIR spectra of all samples show prominent main peak of Ti-O lattice of $TiO_2$ for Ti-O bending mode at 500 – 600 $cm^{-1}$ corresponding to main composition of anatase $TiO_2$ [12].

Corresponding Author E-mail: p_veerachon@hotmail.com 

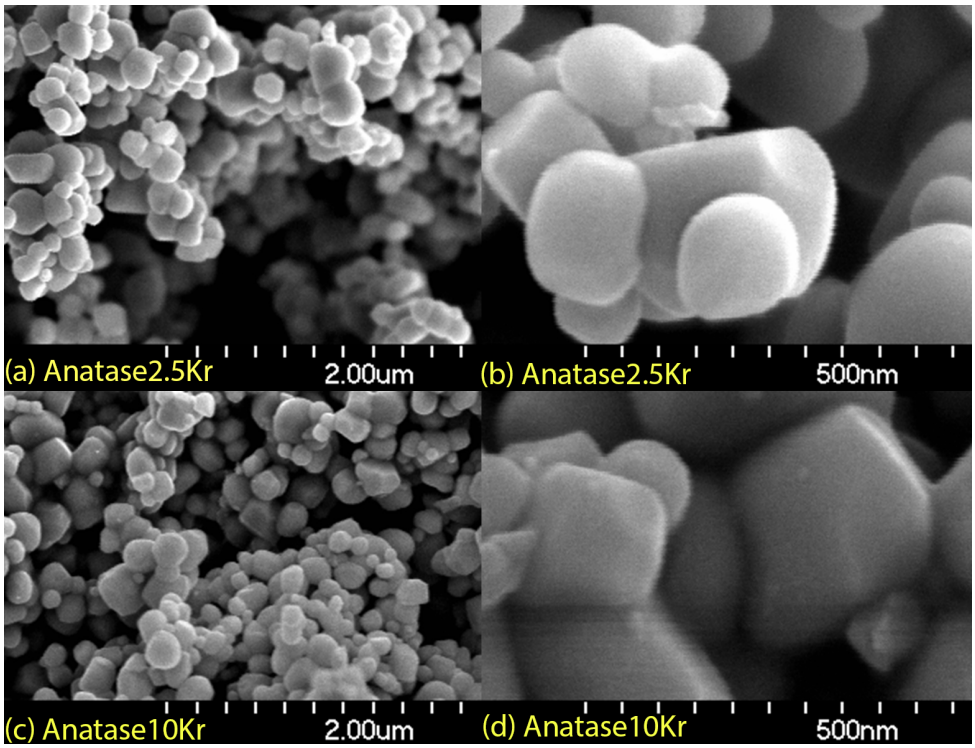


**Fig. 1.** Low and high magnitude FESEM image of (a,b) A-2.5Kr and (c,d) A-10Kr samples.

For the protein characteristic pattern, a low transmittance intensity pattern is assigned to thin layer keratin protein binding at $TiO_2$ surface**.** It also implies the existence of the protein at the surfaces of $TiO_2$ particles**.** Methyl and amide regions are observed as an enlarged IR patterns as shown in Fig**.** 2 **(**b**)** and **(**c**).** The IR pattern of the amide group implies the secondary conformation structure of the protein**.** Vibration energy at around 2966, 2972 and 2853 $cm^{-1}$ are assigned to C-H of $CH_3$ asymmetrical stretching, C-H of $–CH_2$- asymmetrical stretching and $CH_2$ symmetrical stretching, respectively **[**13]. A slightly different methyl peak centroid between A-2.5Kr and A-10Kr is probably due to different protein structure conformations. The difference C-H conformation of adsorbed protein structure may be due to different alkali ratio and/or different protein concentrations which may lead to different interaction side between C-H groups of adsorbed protein with $TiO_2$ surface.

Amide I and II which corresponds to the peaks around 1652 $cm^{-1}$ of A-2.5Kr and A-10Kr and 1492 $cm^{-1}$ of A-2.5Kr [14, 15] are clearly observed**.** The vibration peak at 1432 $cm^{-1}$ which deviates between amide II and III indicates the existence of N-N and/or C-N bond conformation due to bonding with $TiO_2$ surface**.** The amide I peaks present peak centroid and shape which resemble secondary protein of random coil structure and probably combines with small degree of $\beta$-sheet structure**.** Both keratin protein characteristics of methyl and amide compared with bare anatase $TiO_2$ particle proves that the keratin protein could be adsorbed on $TiO_2$ surface in both A-2.5Kr and A-10Kr samples**.** The peak at 1052 $cm^{-1}$ is attributed to stretching mode of sulfonate S-O or S=O that may arise from disulfide bond cleavage and interaction with $TiO_2$ surface**.**

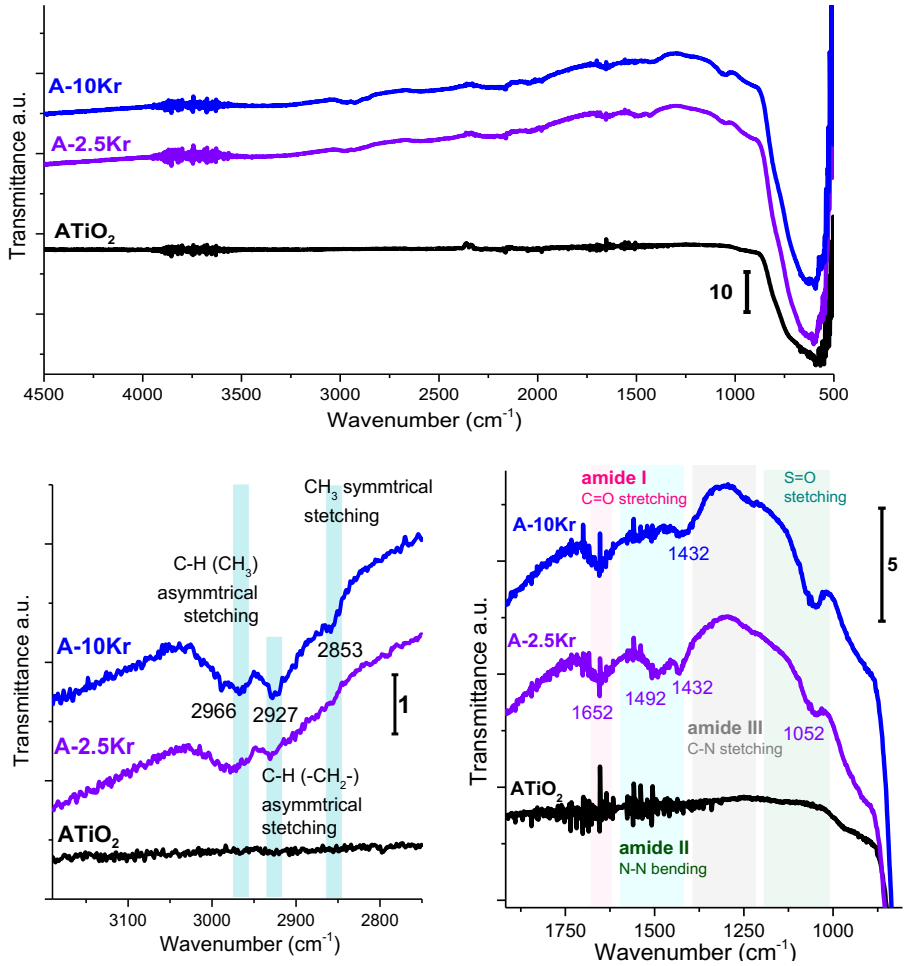


**Fig. 2.** ATR-FTIR spectra A-10Kr, A-2.5Kr samples and the starting anatase $TiO_2$.

Survey scan XPS spectra of A-10Kr, A-2.5Kr samples and the anatase $TiO_2$ as presented in Fig. 3 further reveal interactions between the protein and $TiO_2$ surface. The survey XPS spectra are able to determine the main elements O and Ti corresponding to the main composition of anatase $TiO_2$ without significant impurity element. The high resolution at C*1s*, O*1s*, Ti*2p*, and N*1s* were examined for $TiO_2$ and biomolecule bonds environment. Curve fitted XPS spectra of A-10Kr and A-2.5Kr samples at C*1s* were performed according to carbon bond binding energy of proteins and adsorbed carbon impurity as shown in Fig. 4 **(a).** The main peak positioned at 284.8 eV ascribes to C-C and C-H bonds. The higher binding energy peaks at 288.6 eV may correspond to the C=O, N-C=O groups and at around 285.9-286.7 eV may correspond to the C-N, C-O-H groups of the protein in the A-10Kr and A-2.5Kr samples. However, the peaks at 285.9 to 288.6 eV also represents in bare anatase $TiO_2$ sample due to adsorbed carbon impurity.

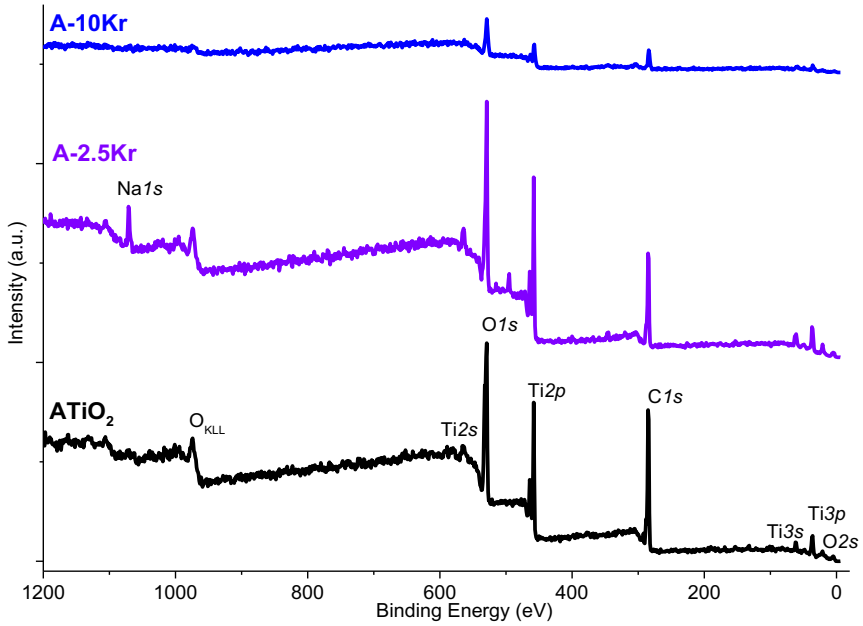


**Fig. 3.** Survey scan XPS spectra of A-10Kr, A-2.5Kr samples and the starting anatase $TiO_2$.

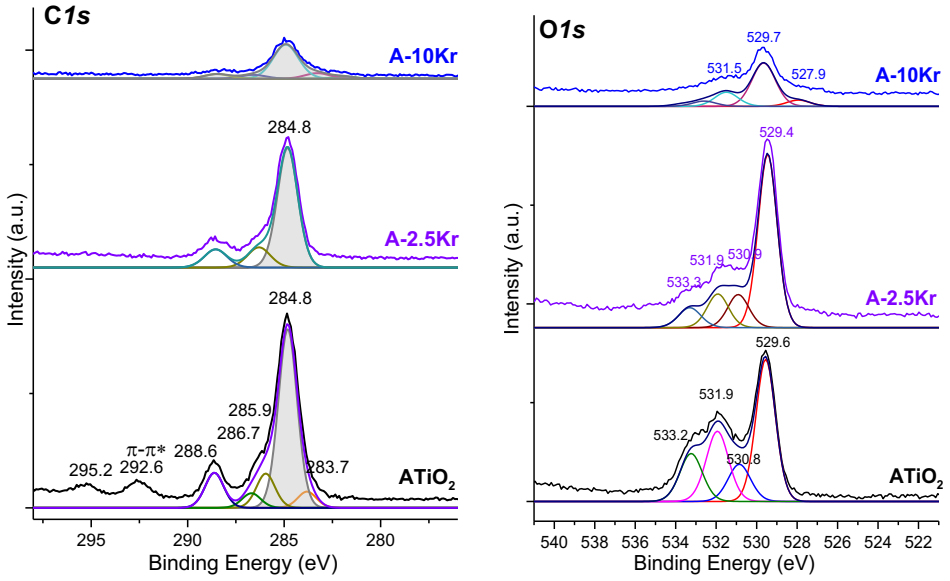


**Fig. 4.** High resolution XPS spectra of A-10Kr, A-2.5Kr samples and the starting anatase $TiO_2$ at the region of (a) C*1s* and (b) O*1s*.

The fitting curve of O*1s* spectra also indicates the main composition of Ti-O-Ti oxygen in $TiO_2$ lattice at around 529.6 eV of bare anatase $TiO_2$ as exhibited in Fig. 4 (b). The O*1s* oxygen in the lattice of A-2.5Kr shifts toward lower binding energy accounting for oxygen around oxygen vacancy site of surface defect which may be induced by alkali solution. The shift to 529.7 of A-10Kr indicates lattice surface oxygen bonding with protein [11,12]. Bonding environment of keratin protein, such as O=C-N, C=O/O-C-H and C-O/$H_2O$ typically appear around 530.9, 531.8 and 533.3 eV which are surprisingly noticed in bare anatase $TiO_2$.

As depicted in Fig. 5 (a), Ti*2p* spin orbit energy splitting component of Ti$2p_{1/2}$ and Ti$2p_{3/2}$ for $TiO_2$ at around 5.7 eV for A-10Kr. A-2.5Kr samples and the starting anatase $TiO_2$ is observed in Ti$2p_{3/2}$ showing binding energy peaks around 458.4 eV [17]. The main Ti$2p_{3/2}$ peak shows only main composition of $Ti^{4+}$ in $TiO_2$ lattice environment that is in good agreement with other results while this value in A-2.5Kr shifts to 458.3 eV due to surface oxygen vacancy that is in accordance with the result from O*1s* spectra.

There is no significant signal of sulfur since a typical sulfur signal in protein was disappeared during dissolution in alkali solution. However, the N1s photoelectron appears in A-10Kr and A-2.5Kr samples showing the relevant evidence of amino protein –$NH_2$, –NH– and –N= at surface particle at binding energy of 400.0 eV [16,18,19]. The electrochemical capacitance behavior of A-10Kr and A-2.5Kr samples were performed by cyclic voltammetry and the curves of different scan rates are represented in Fig. 6 (a) and (b) for capacitance retention profiles. The CV shapes and current density property of A-10Kr and A-2.5Kr samples are compared in Fig.7 for 100 mV/s indicating that CV profile of A-2.5Kr shows redox peaks when compared with A-10Kr.

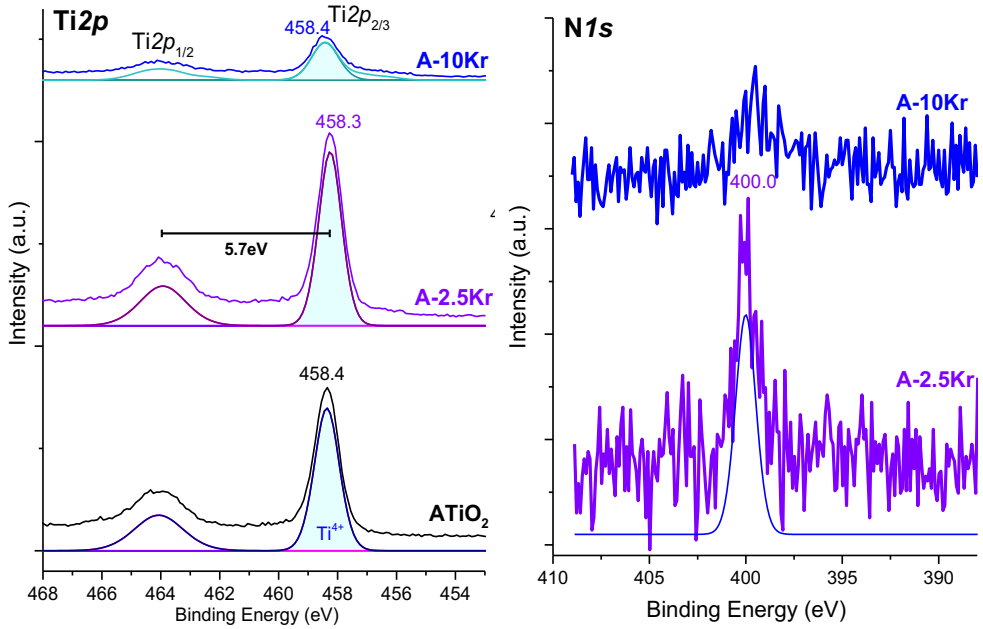


**Fig. 5.** High resolutions XPS spectra of A-10Kr, A-2.5Kr samples and the starting anatase $TiO_2$ in the region of (a) Ti*2p* and (b) N*1s*.

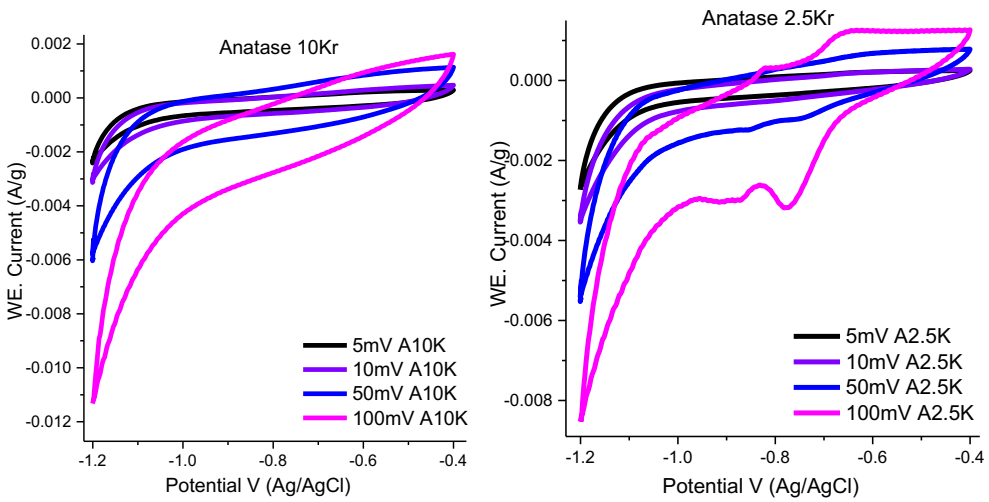


**Fig. 6.** Cyclic voltammmogram curves of (a) A-10Kr and (b) A-2.5Kr samples with different scan rates soaked in 1.0 M KCl electrolyte.

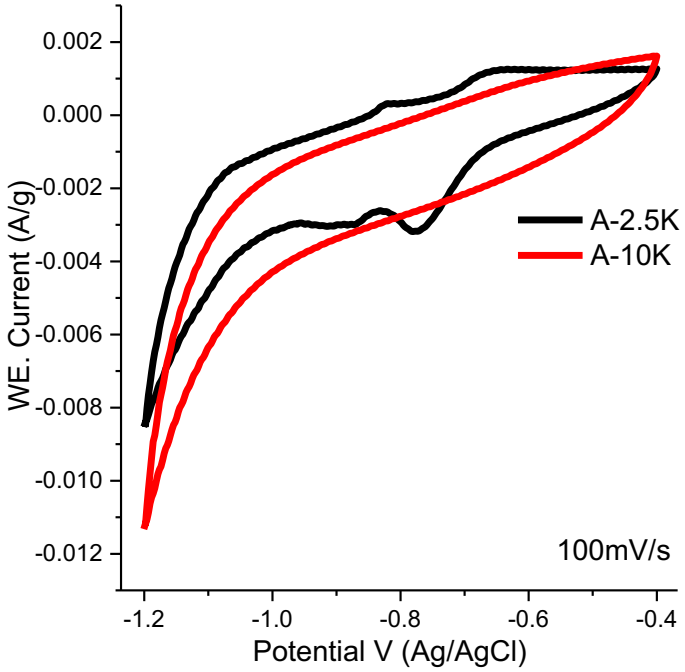


**Fig. 7.** Cyclic voltammogram curves of A-10Kr and A-2.5Kr samples measured at a scan rate of 100 mV/s in 1.0 M KCl electrolyte solution.

## 4. Conclusion

Keratin protein was conjugated to $TiO_2$ surface in the form of secondary random coil conformation structure by bonding via methyl, carbonyl and amine groups. Keratin protein concentration and alkali are considered as the major parameters that have strong effect on adsorbed protein structure conformation behavior and corresponding electrochemical property. $TiO_2$ nanohybrid material showed prominent property with feasibility for advance supercapacitor and bioelectronics technology.

## Acknowledgments

The authors would like to thank Suan Dusit University for support of this work**.**

## References

[1] M.-E. Aubin-Tam and K. Hamad-Schifferli, Structure and function of nanoparticle–protein conjugates, Biomed. Mater. 3 (2008) 034001.

[2] A. O. Elzoghby, A. L. Hemasa, M. S. Freag, Hybrid protein-inorganic nanoparticles: From tumor-targeted drug delivery to cancer imaging, J. Control. Release. 243 (2016) 303-322.

[3] A. Kaushik, R. Kumar, S. K. Arya, M. Nair, B. D. Malhotra and S. Bhansali, Organic−Inorganic Hybrid Nanocomposite-Based Gas Sensors for Environmental Monitoring, Chem. Rev. 115 (2015) 4571-4606.

[4] M. Khairy and S. A. El-Safty, Hemoproteins–nickel foam hybrids as effective supercapacitors, Chem. Commun. 50 (2014) 1356-1358.

[5] A. Vallee, V. Humblot, C.-M. Pradier, Peptide Interactions with Metal and Oxide Surfaces, Acc. Chem. Res. 43 (2010) 1297-1306.

[6] G. Liu, H. G. Yang, J.Pan, Y. Q. Yang, G. Q. (M.) Lu, H.-M. Cheng, Titanium Dioxide Crystals with Tailored Facets, Chem. Rev. 114 (2014) 9559–9612.

[7] N. Rahimi, R. A. Pax, E. M.A. Gray, Review of functional titanium oxides. I: $TiO_2$ and its modifications, Prog. Solid State Chem. 44 (2016) 86-105.

[8] T. Rajh, N. M. Dimitrijevic, M. Bissonnette, T. Koritarov, V. Konda, Titanium Dioxide in the Service of the Biomedical Revolution, Chem. Rev. 114 (2014) 10177–10216.

[9] A. Shavandi, T. H. Silva, A. A. Bekhit, A. El-Din A. Bekhit, Keratin: dissolution, extraction and biomedical application, Biomater. Sci. 5 (2017) 1699-1735.

[10] B. J. G. E. Pieters, M. B. v. Eldijk, R. J. M. Nolte, J. Mecinović, Natural supramolecular protein assemblies, Chemical Society Reviews, 45 (2015) 24-39.

[11] J. M. Galloway and S. S. Staniland, Protein and peptide biotemplated metal and metal oxide nanoparticles and their patterning onto surfaces, J. Mater. Chem. 22 (2012) 12423-12434.

[12] G. Liu, L. Liu, J. Song, J. Liang, Q. Luo, D. Wang, Visible light photocatalytic activity of $TiO_2$ nanoparticles hybridized by conjugated derivative of polybutadiene, Superlattices Microstruct. 69 (2014)164-174.

[13] M. G. Sowa, J. Wang, C. P. Schultz, M. K. Ahmed, H. H. Mantsc, Infrared spectroscopic investigation of in vivo and ex vivo human nails, Vib. Spectrosc. 10 (1995) 49-56.

[14] J. J. Martin, J. M. Cardamone, P. L. Irwin, E. M. Brown, Keratin capped silver nanoparticles – Synthesis and characterization of a nanomaterial with desirable handling properties, Colloids Surf., B. 88 (2011)354-361.

[15] A. Shavandi, A. Carne, A. A. Bekhit, A. E.-D. A. Bekhit, An improved method for solubilisation of wool keratin using peracetic acid, J. Environ. Chem. Eng. 5 (2017) 1977-1984.

[16] C. Gruian, E. Vanea, S. Simon, V. Simon, FTIR and XPS studies of protein adsorption onto functionalized bioactive glass, Biochim. Biophys. Acta. 1824 (2012) 873–881.
[17] K. L. Syres, A. G. Thomas, W. R. Flavell, B. F. Spencer, F. Bondino, M. Malvestuto, A. Preobrajenski, M. Grätzel, Adsorbate-Induced Modification of Surface Electronic Structure: Pyrocatechol Adsorption on the Anatase $TiO_2$ (101) and Rutile $TiO_2$ (110) Surfaces, J. Phys. Chem. C. 116 (2012) 23515–23525.
[18] I. N. Shabanova, I. V. Menshikov, N. S. Terebova, A. S. Terent'ev, Investigation of the interatomic interaction in immunoglobulin G fragments via X-ray photoelectron spectroscopy, J. Surf. Invest.: X-Ray, Synchrotron. 11 (2017) 823–826.
[19] Y. K. Gao, F. Traeger, K. Kotsisb, V. Staemmler, A theoretical study of the XP and NEXAFS spectra of alanine: gas phase molecule, crystal, and adsorbate at the ZnO(1010) surface, Phys. Chem. Chem. Phys. 13 (2011) 10709-10718.